

## The vibrational spectrum of synthetic hydrogrossular (katoite) $\text{Ca}_3\text{Al}_2(\text{O}_4\text{H}_4)_3$ : A low-temperature IR and Raman spectroscopic study

BORIS A. KOLESOV<sup>†</sup> AND CHARLES A. GEIGER\*

Institut für Geowissenschaften, Universität Kiel, Olshausenstrasse 40, D.24098 Kiel, Germany

### ABSTRACT

The powder IR spectra of synthetic hydrogrossular,  $\text{Ca}_3\text{Al}_2(\text{O}_4\text{H}_4)_3$ , were recorded at temperatures between 298 and 10 K and the polarized single-crystal Raman spectra at 298 and 4 K. The results were interpreted using factor group analysis which predicts the number and symmetry of the different IR- and Raman-active modes. A first attempt was made to assign the observed bands in the IR and Raman spectra to various atomic or polyhedral motions and to make a first-order lattice dynamic analysis. The mode assignments for grossular,  $\text{Ca}_3\text{Al}_2(\text{SiO}_4)_3$ , and hydrogrossular were compared. The measured spectra are considerably different in the high-wavenumber region, where O-H stretching modes occur, between 298 and 10/4 K. In the Raman spectra two different symmetry O-H bands are observed at  $3648\text{ cm}^{-1}$  ( $A_{1g} + E_g$ ) and  $3653\text{ cm}^{-1}$  ( $F_{2g}$ ) at room temperature, while at 4 K several O-H bands are present. At room temperature an IR-active O-H band located around  $3662\text{ cm}^{-1}$  narrows and shifts to higher wavenumbers and also develops structure below about 80 K. Concomitantly, several weak intensity O-H bands located around  $3600\text{ cm}^{-1}$  begin to appear and they become sharper and increase in intensity with further decreases in temperature down to 10 K. The spectra indicate that the vibrational behavior of individual OH groups and their collective interactions measurably affect the lattice dynamic (i.e., thermodynamic) behavior of hydrogrossular. The  $(\text{O}_4\text{H}_4)$  group in garnet is best described as a “chemical component” that can substitute for  $\text{SiO}_4$  tetrahedra and not as a “structural or polyhedral unit”. The line widths of the IR and Raman O-H bands at low and room temperature were interpreted qualitatively based on the time scales associated with the Raman and IR experiment, which are different in magnitude. The results of this study demonstrate the need for making spectroscopic measurements at low temperatures when studying the vibrational behavior of O-H modes in minerals.

### INTRODUCTION

There is great current interest in understanding interactions, especially at the atomistic or molecular level, between  $\text{H}_2\text{O}$  and its components (e.g.,  $\text{H}^+$ ,  $\text{OH}^-$ ,  $\text{H}_2$ ,  $\text{O}_2$ ) and Earth materials. Hydrothermal ore deposition, chemical weathering of various materials, and many metamorphic reactions are important examples of the types of processes that are largely controlled by the nature of  $\text{H}_2\text{O}$ -rich fluids and their interplay with solid phases. From a mineralogical or crystal-chemical standpoint, much effort has been made over the past approximately 30 years in investigating how  $\text{OH}^-$  can be incorporated into nominally anhydrous (rock-forming) minerals, or NAMS as they are now often referred to, following early studies by Martin and Donnay (1972) and Wilkins and Sabine (1973), for example. Here, questions such as the bulk water content of the mantle, and what phases can incorporate  $\text{OH}^-$ , and in what concentrations, come immediately to mind. Thus, a good deal of research has focused on pyroxene, olivine, and garnet (e.g., Bell and Rossman 1992). All of these silicates are capable of incorporating

small concentrations of  $\text{OH}^-$  at mantle conditions. However, in spite of the amount of research that has been done, it is still poorly understood where the  $\text{OH}^-$  is located in their structures or through what substitution mechanism(s) it has been incorporated. In this regard, the hydrogarnet substitution (i.e.,  $\text{O}_4\text{H}_4 \leftrightarrow \text{SiO}_4$ ) has received special attention, because it is a verified mechanism for incorporating of  $\text{OH}^-$  in garnet (Cohen-Addad et al. 1967; Foreman 1968; Lager et al. 1987; Ambruster and Lager 1989) and possibly in other silicates as well. Indeed, at relatively low geologic temperatures there is complete solid solution between grossular,  $\text{Ca}_3\text{Al}_2(\text{SiO}_4)_3$ , and hydrogrossular,  $\text{Ca}_3\text{Al}_2(\text{O}_4\text{H}_4)_3$ , as was shown a number of years ago by Flint et al. (1941). It can be stated that this substitution offers a simple starting point for investigating and understanding the crystal-chemical nature of  $\text{OH}^-$  in NAMS.

The primary experimental tool that is used in this type of study has been single-crystal IR spectroscopy. Raman spectroscopy has also been used but to a lesser degree. However, because the IR spectra of natural garnets are often quite complicated, inasmuch as they show a plethora of different spectra (see Rossman and Aines 1991 for grossular-hydrogrossular garnets as an example), work on compositionally simple garnets (pyrope, almandine, grossular, and nearly end-member compositions) that have been synthesized hydrothermally under controlled conditions (Geiger

\* E-mail: chg@min.uni-kiel.de

<sup>†</sup> Permanent address: Institute of Inorganic Chemistry, Russian Academy of Science, Lavrentiev prosp. 3, Novosibirsk 630090, Russia.

et al. 1991, 2000; Hösch and Langer 1996; Geiger and Armbruster 1997) is essential. Single-crystal IR measurements done at different temperatures show that most synthetic garnets have relatively simple spectra compared to their natural counterparts. But here, too, the spectra are not completely interpretable (Geiger et al. 2000). In spite of all the experimental work that has been done, little is understood of how OH<sup>-</sup> is structurally incorporated in nominally anhydrous silicates. Two major obstacles exist in interpreting vibrational spectra more quantitatively. First, no solid theoretical factor-group analysis has been made that would allow one to predict how many OH<sup>-</sup> modes should occur in the case of the hydrogarnet substitution and what their symmetries should be (see, however, Harmon et al. 1982). Second, there is an absence of vibrational spectroscopic measurements made at very low temperatures. This is often necessary (see for example Kolesov and Geiger 2000, 2002), because the hydrogen atom generally has large vibrational amplitudes and this leads to extensive O-H mode broadening. Indeed, thermal anharmonicity and a small degree of dynamic O-H mode splitting has been observed in the IR spectra of OH<sup>-</sup>-containing garnets recorded between 298 and about 80 K (Geiger et al. 1991, 2000; Hösch and Langer 1996). As a result of these deficiencies, and although hundreds of IR spectra of various natural OH<sup>-</sup>-bearing garnets have been collected over the years, spectral interpretations and the classification of various “OH-bearing garnet types” based on their “IR signature” are purely empirical in nature (e.g., Rossman and Aines 1991; Matsyuk et al. 1998).

To better understand the crystal chemistry, the hydrogarnet substitution mechanism, and the vibrational spectrum of OH<sup>-</sup>-bearing garnets, we have obtained powder IR and polarized single-crystal Raman data from synthetic hydrogrossular. The measurements were made from room temperature down to very low temperatures (10 or 4 K) to understand, for example, the behavior of the internal O<sub>4</sub>H<sub>4</sub> stretching modes. In addition, the spectra are interpreted using the first complete factor-group analysis made for hydrogrossular.

## EXPERIMENTAL METHODS

### Synthesis and spectroscopic measurements

Hydrogrossular was synthesized hydrothermally in Tuttle-type rod vessels. To begin, high purity CaCO<sub>3</sub> and Al<sub>2</sub>O<sub>3</sub> powders in the molar proportions 3:1 were intimately ground and mixed, pressed into pellets, and then sintered at high temperatures for several days to produce Ca<sub>3</sub>Al<sub>2</sub>O<sub>6</sub>. About 100 mg of this compound was welded, together with abundant distilled H<sub>2</sub>O, into Au capsules of 5 mm diameter and placed into rod vessels. The synthesis conditions were 250 °C and 3 Kbar water pressure and the experiments were done for a period of 2 weeks. The resulting product was largely a fine white powder consisting mostly of very tiny hydrogrossular crystals less than 10 μm in diameter. Within the fine powder, a small number of euhedral and mostly transparent larger garnet crystals, approximately 50 to about 200 μm in diameter, were observed. An X-ray powder diffraction measurement of the synthetic product revealed peaks that could only be indexed to hydrogrossular.

Powder transmission IR measurements were made using a Bruker FT-IFS66 spectrometer equipped with an MCT detector. About 1 mg of hydrogrossular was ground and mixed with about 300 mg KBr and pressed under vacuum to a transparent pellet of 13.0 mm diameter. The low-temperature spectra were recorded using a cold finger-type He closed-cycle cryostat attached to the spectrometer. The precision of the temperature control is about ±1 K. Spectra were collected from 300 down to 10 K every 20 or 10 K. A total of 32 scans was recorded at a resolution of 2 cm<sup>-1</sup> and merged for the final spectrum.

The single-crystal Raman measurements were performed with a Triplemate

SPEX spectrometer with a CCD detector, model LN-1340 PB, from Princeton Instruments. The 514.5 or 488 nm lines of an Ar laser were used for the spectral excitation. The low (4 K) and room temperature (298 K) spectra were measured in 180° collection geometry with a microscope. The 4 K spectra were recorded by fixing one of the larger euhedral hydrogrossular crystals on a cold finger of a helium cryostat “MicrostatHe” from the company Oxford Instruments. The precision of the measured temperatures is estimated to be ±1 K, while the accuracy is less. Measurements were performed with a spectral resolution of 2 cm<sup>-1</sup> at 4 K and 5 cm<sup>-1</sup> at room temperature. The polarized room temperature single-crystal spectra were taken from the (110) face, which has a rhombic shape, of a single crystal with parallel (*A<sub>1g</sub>* and *E<sub>g</sub>*) and cross (*F<sub>2g</sub>*) polarizations of the incident and scattered light. The 4 K Raman spectra were recorded with restricted crystal orientation because of physical limitations imposed by the cryostat and because of difficulties in exactly orientating the small crystal.

Fitting of the spectra was done to obtain information on the line widths (FWHM) of some bands. This was done with the program Origin 7.0 using Lorentzian line shapes.

## RESULTS

### Structure and factor-group analysis of hydrogrossular

The space group of hydrogrossular is *Ia* $\bar{3}d$ , with *Z* = 8 at room temperature (Cohen-Addad et al. 1967; Foreman 1968; Lager et al. 1987). A polyhedral model of the structure is shown in Fig. 1, based on data from the last reference. The Ca and Al cations are located at special crystallographic positions with *D*<sub>2</sub> and *C*<sub>3i</sub> point symmetry, respectively, and the oxygen and hydrogen atoms are at general positions. The individual OH<sup>-</sup> groups build an O<sub>4</sub>H<sub>4</sub> tetrahedron of *S*<sub>4</sub> symmetry with the oxygen atoms located at the four corners. The center of the tetrahedron is empty. The two crystallographically independent O...O distances lie between 3.052 and 3.244 Å at 100 K and 3.058 and 3.245(2) Å at 300 K (Lager et al. 1987). One hydrogen atom is bonded to one oxygen atom with an O-H bond length of approximately 0.95

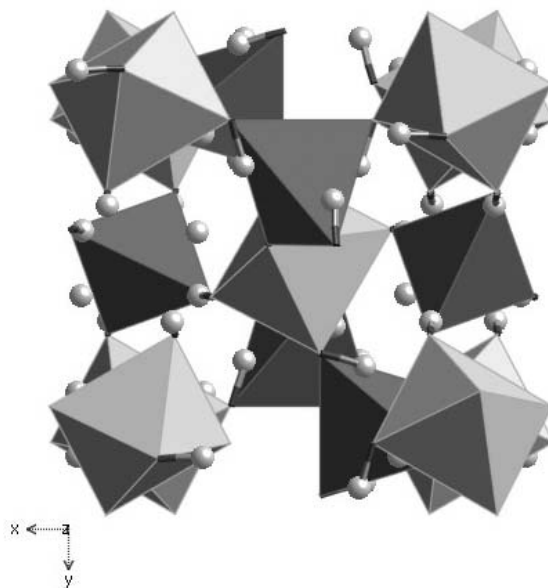


**FIGURE 1.** Polyhedral structure model of hydrogrossular. The H atoms are shown by the small dark spheres and form together with the O atoms O<sub>4</sub>H<sub>4</sub> tetrahedra. The AlO<sub>6</sub> octahedra, which are corner shared with the tetrahedra, are lightly shaded. The Ca atoms are not shown and some atoms have been removed for the sake of clarity.

Å. The hydrogen atoms show large vibrational displacements perpendicular to the O-H bond and the H atoms can, upon vibration, penetrate into the tetrahedron, but spend most of their time slightly above the faces of the tetrahedra (Lager et al. 2002). The OH vector bisects approximately each tetrahedral face. The point symmetry of an  $O_4H_4$  tetrahedron in the lattice is  $S_4$ . Figure 2 depicts a symmetry analysis for vibrations of a single isolated OH molecular unit, their transformation to point symmetry  $C_1$  in a  $(O_4H_4)$  cluster, and finally for a complete  $(O_4H_4)$  cluster of  $S_4$  symmetry. The  $(O_4H_4)$  group vibrations consist of four symmetry types, namely  $A$ ,  $B$ ,  $E(1)$ , and  $E(2)$  (Fig. 3), each containing 6 total vibrations. Each symmetry type contains one  $O_4H_4$ -stretching, three  $O_4H_4$ -translation ( $x, y, z$ ) and two  $O_4H_4$ -libration ( $x, y$ ) vibrations. The various internal  $(O_4H_4)$  stretching modes, as derived from this symmetry analysis, are given by the crystal space group symmetry and the dynamical interactions between the different modes. Table 1 lists the number and symmetry of all the vibrational modes for hydrogrossular. The  $A_{1g}$ ,  $E_g$ , and  $F_{2g}$  gerade modes are Raman active. The  $F_{1u}$  modes are IR active. One of the three T(OH) modes of  $A_{1g}$  symmetry, where all the OH groups move in-phase around some axis, should generate a librational mode of a  $(O_4H_4)$  tetrahedron analogous to a R(SiO<sub>4</sub>)

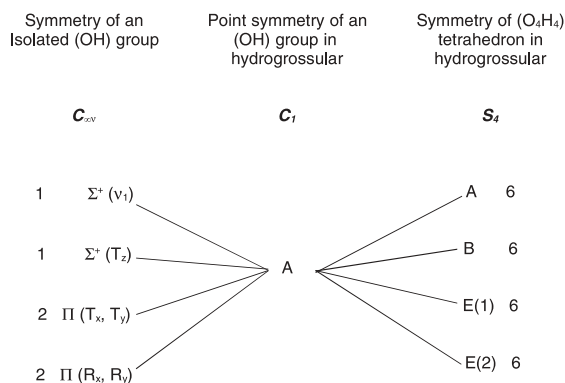


FIGURE 2. Correlation scheme for the vibrations of the  $(O_4H_4)$  tetrahedron in hydrogrossular.

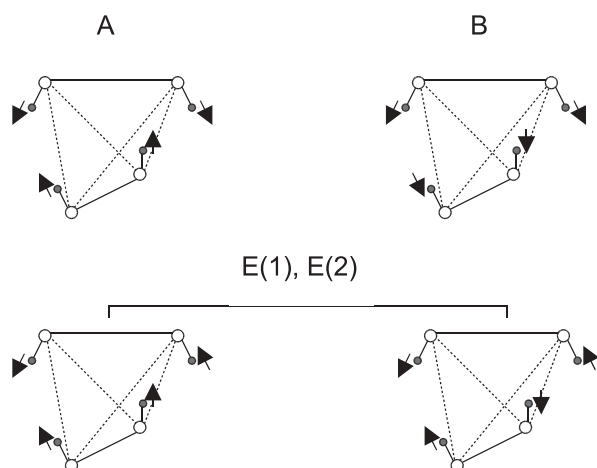


FIGURE 3. Depiction of the various vibrational modes of different symmetry for an  $(O_4H_4)$  tetrahedron in hydrogrossular.

mode of  $A_{1g}$  symmetry in silicate garnet (see Kolesov and Geiger 1998). Translational modes of the  $O_4H_4$  groups should appear in the  $E_g$  and  $F_{2g}$  spectra.

### IR and Raman spectra

Figure 4 shows the powder infrared absorption spectrum of hydrogrossular between 500 and 4500  $cm^{-1}$  at room temperature. Strong “lattice modes” are observed at the lower wavenumbers, as is a single intense internal O-H stretching band at 3662  $cm^{-1}$  (Rossman and Aines 1991) and also a broad absorption feature at roughly 3450  $cm^{-1}$ . Figure 5 shows a stacked plot of IR spectra in the wavenumber region of the O-H stretching vibrations from 298 to 10 K. It documents a narrowing and the development of structure for the broad band at 3662  $cm^{-1}$  and its shift to higher wavenumbers and also the concomitant appearance of several weak O-H bands located around approximately 3600  $cm^{-1}$  with decreasing temperature. At 10 K, the main band envelope consists of an intense band at 3683  $cm^{-1}$  and several poorly resolved components at slightly higher and lower wavenumbers. These are expressed by slight shoulders that develop in a regular fashion upon cooling below 80 K.

The polarized single-crystal Raman spectrum of hydrogrossular at room temperature is shown in Figures 6a ( $A_{1g} + E_g$ ) and 6b ( $F_{2g}$ ). The observed bands are slightly broadened compared to those observed for silicate garnets (Kolesov and Geiger 1998). Two different symmetry O-H bands are observed at 3648  $cm^{-1}$

TABLE 1. Symmetry analysis of the vibrations in hydrogrossular

	Ca	Al	T(OH)	R(OH)	(O-H) <sub>stretch</sub>	Activity
$A_{1g}$	–	–	3	2	1	Raman
$A_{2g}$	1	–	3	2	1	
$E_g$	1	–	6	4	2	Raman
$F_{1g}$	3	–	9	6	3	
$F_{2g}$	2	–	9	6	3	Raman
$A_{1u}$	–	1	3	2	1	
$A_{2u}$	1	1	3	2	1	
$E_u$	1	2	6	4	2	
$F_{1u}$	3*	3*	9*	6	3	IR
$F_{2u}$	2	3	9	6	3	

\* One  $F_{1u}$  mode should be subtracted as an acoustic vibration.

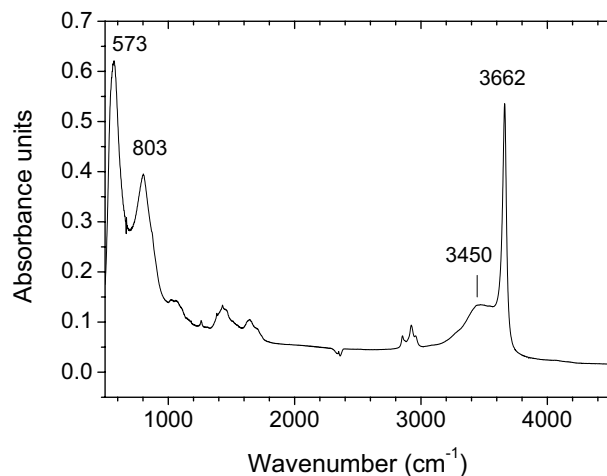


FIGURE 4. Room-temperature powder infrared absorption spectrum of hydrogrossular. An O-H stretching band is located at 3662  $cm^{-1}$  and two low energy lattice vibrations at 803 and 573  $cm^{-1}$ .

( $A_{1g} + E_g$ ) and at  $3653 \text{ cm}^{-1}$  ( $F_{2g}$ ). Figure 7a shows the low-energy lattice modes between 100 and  $1000 \text{ cm}^{-1}$  for an approximate Raman ( $aa$ )-spectrum at 4 K (The tiny crystal could not be orientated exactly). At 4 K, all the bands are narrower and shifted by approximately  $10\text{--}20 \text{ cm}^{-1}$  to higher energy compared to the 298 K spectrum, except for the mode at  $334 \text{ cm}^{-1}$ , which shifts very little. The mode at  $231 \text{ cm}^{-1}$  at room temperature appears to split into two bands at 222 and  $259 \text{ cm}^{-1}$  at low temperature. Figure 7b shows the high wavenumber region in detail and here several different O-H modes can be observed. The O-H stretching region can be described, as in the case for the low temperature

IR spectra, as consisting of two O-H-band-containing subregions centered roughly around  $3580$  and  $3670 \text{ cm}^{-1}$ . The high-wavenumber subregion shows 6 modes of greatly differing intensity. The various lower energy modes around  $3580 \text{ cm}^{-1}$  occurring at 4 K are not observed in the spectra at 298 K. The results of fitting the Raman spectrum in the O-H stretching region and the most intense OH IR band envelope at temperatures of 298 and 10 K are given in Table 2. The number of fitted IR bands is considered an estimate and may not be exactly correct. This is a result of the strong overlapping between the individual absorption lines. The individual band widths (i.e., FWHH) are largely independent of the exact number of bands used in the fit. Unpolarized Raman spectra are presented in Figure 8 as a function of temperature in the low-wavenumber region and they show lower energy lattice vibrations. No overt changes in the spectra are observed.

## DISCUSSION

This study presents very low temperature (i.e.,  $<80 \text{ K}$ ) IR and Raman spectra of hydrogrossular. Several interesting phenomena occur, such as the effect of thermal anharmonicity and dynamic mode splitting for the internal  $\text{O}_4\text{H}_4$ -stretching modes. The experimental spectroscopic data, in combination with the theoretical factor-group analysis, also allow a first analysis of the vibrational spectrum of hydrogrossular. The results have im-

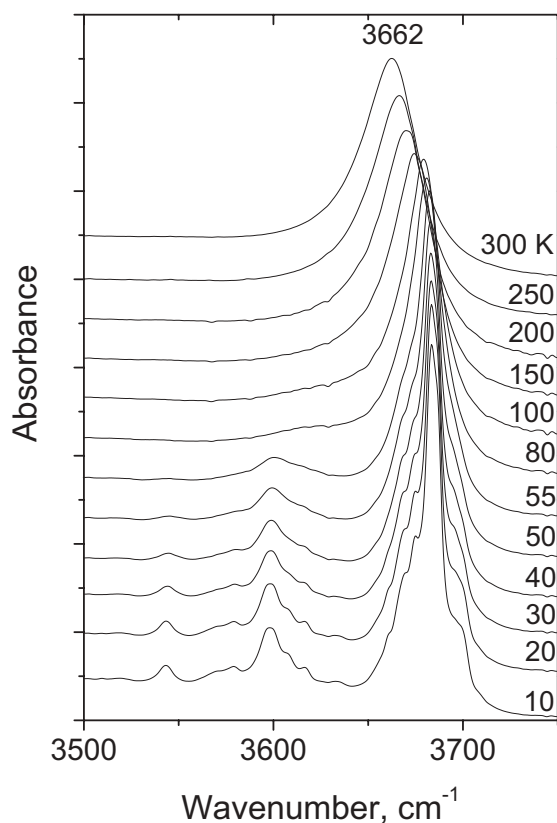


FIGURE 5. Powder temperature-dependent IR spectra showing O-H stretching vibrations in hydrogrossular. Note the fine structure developing on the most intense band below about 50 K.

TABLE 2. Line widths (FWHH in  $\text{cm}^{-1}$ ) of various O-H stretching bands (in  $\text{cm}^{-1}$ ) in the Raman and IR spectra of hydrogrossular at 10/4 K and 298 K

	Band	Symmetry	FWHH	
			10/4 K	298 K
IR	3655	$F_{1u}$	16.2	
	3660	—	5.8	
	3668	—	10.4	
	3675	—	7.8	
	3683	—	7.4	
	3687	—	4.7	
	3694	—	5.7	
	3697	—	6.1	
	3701	—	5.8	
	3661	$3F_{1u}$		32.5
	Raman	3648		2.5
3659			2.6	
3670			4.0	
3674			4.5	
3683			2.2	
3699			2.0	
3648		$A_{1g} + 2E_g$		38.7
3653		$3F_{2g}$		39.9

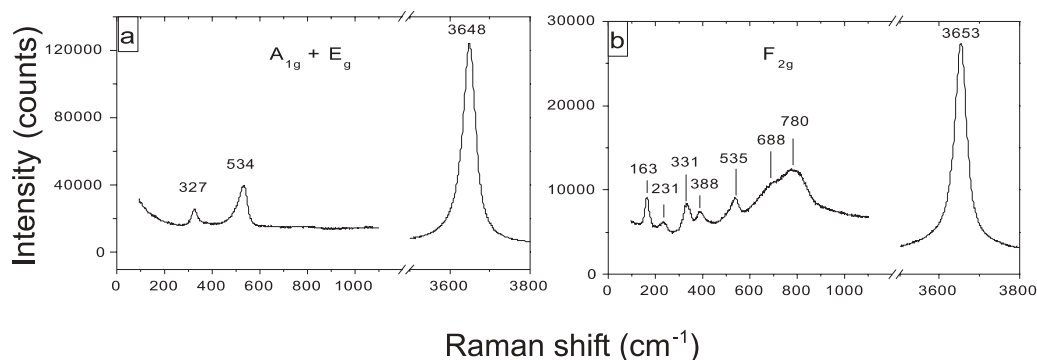


FIGURE 6. Polarized single-crystal Raman spectra of hydrogrossular at room temperature. (a) ( $A_{1g} + E_g$ )-spectrum. (b)  $F_{2g}$ -spectrum.

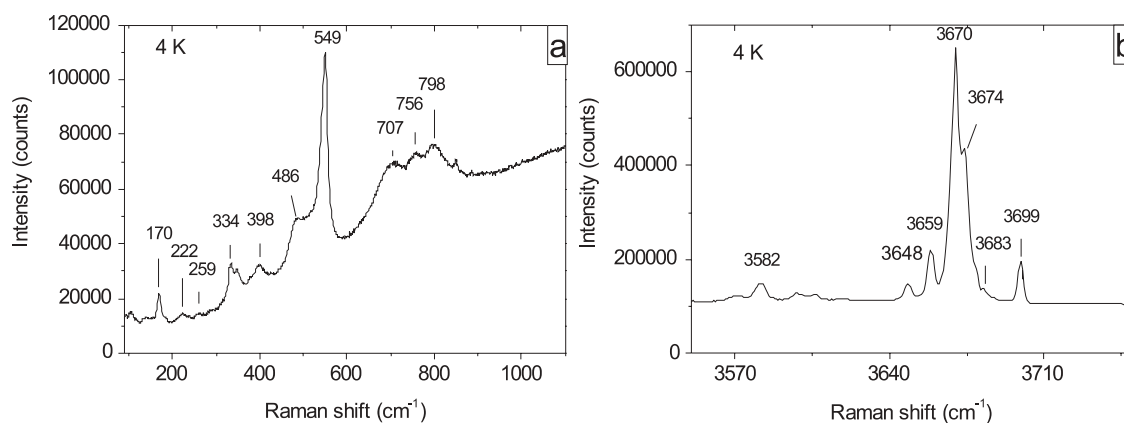


FIGURE 7. Unpolarized Raman spectra of hydrogrossular in the low and high wavenumber regions at 4 K.

plications for the study of OH<sup>-</sup> in nominally anhydrous silicate garnets and perhaps in other NAMS as well. We will consider first the vibrational spectrum of hydrogrossular.

The Raman spectrum of hydrogrossular should consist of (1) Ca-motions, (2) external T- and R(librational)-modes of (O<sub>4</sub>H<sub>4</sub>) clusters [here, it should be clearly noted that it is certain combinations of translational OH motions that give rise to external T(O<sub>4</sub>H<sub>4</sub>)- and R(O<sub>4</sub>H<sub>4</sub>)-type tetrahedral modes], and (3) internal O-H stretching modes deriving from the O<sub>4</sub>H<sub>4</sub> groups. The following points are important for a first-order lattice-dynamic analysis: the wavenumbers of the Ca modes in hydrogrossular should not be greatly different from the Ca modes in grossular and andradite that are located between 240 and 320 cm<sup>-1</sup> (Kolesov and Geiger 1998). The T(O<sub>4</sub>H<sub>4</sub>) and R(O<sub>4</sub>H<sub>4</sub>) vibrations in hydrogrossular result from collective vibrations of individual OH<sup>-</sup> units and, thus, are different in nature compared to external vibrations of strongly bonded SiO<sub>4</sub> groups in silicate garnets. Therefore, the energies of T(O<sub>4</sub>H<sub>4</sub>) and R(O<sub>4</sub>H<sub>4</sub>) modes should be similar and mixed. This is not the case for individual T(OH) and R(OH) modes, because the former involves the vibration of the OH unit as a whole, while the latter largely involves just the motion of the hydrogen atom. The energy of a R(OH) mode should thus be higher. Based on these considerations, the broad bands between 600–800 cm<sup>-1</sup> (Fig. 7a) are assigned to R(OH) modes of *F<sub>2g</sub>* symmetry (their counterparts with *A<sub>1g</sub>* and *E<sub>g</sub>* symmetry are very weak in intensity for reasons that we do not presently understand). The broad band at 535 cm<sup>-1</sup> in both the *A<sub>1g</sub>* + *E<sub>g</sub>* and *F<sub>2g</sub>* spectra, which partly splits at 4 K (Fig. 8a), is assigned to a T(OH) motion. The band at 327 cm<sup>-1</sup> in the *A<sub>1g</sub>* spectrum should be assigned to a R(O<sub>4</sub>H<sub>4</sub>) motion, because it is the only external mode of the O<sub>4</sub>H<sub>4</sub>-tetrahedron that is allowed in the totally symmetric spectrum [the analogous R(SiO<sub>4</sub>) mode in Ca-containing silicate garnets is located around 360 cm<sup>-1</sup>, Kolesov and Geiger 1998]. The bands at 331 and 388 cm<sup>-1</sup> (*F<sub>2g</sub>*) are mixed T/R(O<sub>4</sub>H<sub>4</sub>) modes. Finally, the bands at 163 and 231 cm<sup>-1</sup> (*F<sub>2g</sub>*), observed at room temperature, are interpreted as Ca vibrations. The reason for the splitting of the band at 231 cm<sup>-1</sup> at 4 K is not completely clear, but it could perhaps indicate a phase change (see below). Finally, we note that coupling and mixing between various modes should occur, as is the case in silicate garnets as well as other silicates (Kolesov and Geiger

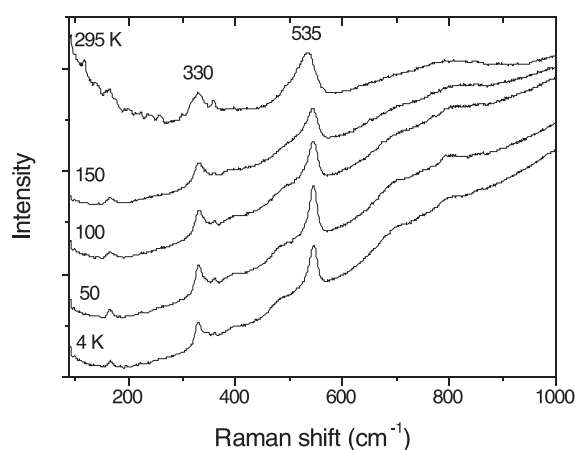


FIGURE 8. Temperature-dependent Raman spectra of hydrogrossular in the wavenumber region of the lattice modes between 4 and 295 K.

1998; Geiger and Kolesov 2002), but they are not considered explicitly and completely in our first-order analysis of the spectra. Thus, “pure vibrations” do not exist in a strict sense. The Raman mode assignments for hydrogrossular are summarized in Table 3 and are compared to those for grossular.

The major difference between the crystal chemistry and lattice-dynamic behavior of silicate garnet and hydrogarnet lies in the nature of their respective tetrahedral sites and this aspect deserves careful analysis. The symmetry of the O-H stretching vibrations is governed by the point symmetry of the (O<sub>4</sub>H<sub>4</sub>) tetrahedron and the space-group symmetry of hydrogrossular. The symmetries of the various internal O<sub>4</sub>H<sub>4</sub> modes in hydrogrossular are depicted in Figure 3. It can be shown that the *A<sub>g</sub>*-symmetry O-H modes derive from an *A*-mode, the *E<sub>g</sub>*-symmetry modes from *A* and *B* modes, and the *F<sub>2g</sub>* and *F<sub>1u</sub>* symmetry modes from *B*, *E*(1), and *E*(2) modes. This follows from the correlation between the irreducible representations of the groups of different symmetry. In terms of Raman activity, one *A<sub>g</sub>* and two *E<sub>g</sub>* Raman modes are represented by the broad band at 3648 cm<sup>-1</sup> in the room-temperature spectrum (Fig. 6a), while the three *F<sub>2g</sub>* modes are represented by the band at 3653 cm<sup>-1</sup> (Fig. 6b). The difference in energy between these two bands is only 5 cm<sup>-1</sup> and this means that dynamical splitting between the O-H modes is

**TABLE 3.** First-order Raman mode assignments for hydrogrossular at room temperature and a comparison to those for grossular

Hydrogrossular		Grossular	
Mode	Wavenumber (cm <sup>-1</sup> )	Mode	Wavenumber (cm <sup>-1</sup> )
(OH) <sub>str</sub>	3648, 3653	(Si-O) <sub>str</sub>	827, 848, 880, 904, 1007
R(OH)	688, 780	(Si-O) <sub>bend</sub>	483, 512, 529, 550, 582, 592, 630
T(OH)	535	R(SiO <sub>4</sub> )	319, 333, 351, 373, 376, 389, 420
T(O <sub>4</sub> H <sub>4</sub> ) + R(O <sub>4</sub> H <sub>4</sub> )	331, 327, 388	T(SiO <sub>4</sub> )	181, 186
T(Ca)	163, 231	T(Ca)	247, 280, 320

very small. From this, it follows that the six highest energy bands (i.e., 3649, 3659, 3670, 3674, 3683, and 3699 cm<sup>-1</sup>) observed in the Raman spectrum at 4 K (Fig. 7b) should be assigned to stretching vibrations of the O<sub>4</sub>H<sub>4</sub> tetrahedra.

In terms of the IR-active modes, the  $F_{1u}$  OH modes should not differ significantly in wavenumber from their Raman-active counterparts and thus should be represented by the broad band at 3662 cm<sup>-1</sup> observed at room temperature (Fig. 5). The center of this band envelope shifts to higher wavenumbers with decreasing temperature and it also develops fine structure. At 10 K, this envelope can be fit with several individual OH bands (whose exact number is difficult to determine), and the number is clearly greater than that predicted by group theory under space group  $Ia\bar{3}d$ . In addition to these high-energy O-H Raman- and IR-stretching modes, several weak bands begin to appear in the IR spectra in the wavenumber range of 3550–3620 cm<sup>-1</sup> (Fig. 6) at temperatures less than 80 K. Their counterparts are seen in the Raman spectrum at 4 K (Fig. 7b). Their assignment is not a simple task. We propose that they are O-H modes that arise through the formation of weak hydrogen bonding, OH...O, within the O<sub>4</sub>H<sub>4</sub> tetrahedra. We think this because the presence of hydrogen bonding should cause a decrease in the wavenumber of O-H stretching modes. It should be noted that the two crystallographic O...O distances in hydrogrossular, 3.058 and 3.245 Å at room temperature (Lager et al. 1987), are such that weak hydrogen bonding could occur. A decrease in temperature should lead to structural contraction and a shortening of the O...O distances and, thus, should increase the strength of any possible hydrogen bonding. A dampening of the large thermal motion of the light H atom may allow for stabilization of hydrogen bonding at the lower temperatures. The number and relative strengths of the hydrogen bonds cannot be easily determined, especially if a phase change occurs at low temperatures and the space group symmetry changes. It is possible that only some H atoms may form weak hydrogen bonding with a neighboring oxygen atom or that variations in hydrogen bonding strength exist within an O<sub>4</sub>H<sub>4</sub> group. This could lead to a distortion from  $S_4$  symmetry, which could explain the presence of more O-H vibrational modes than predicted by group theory under the space group symmetry of  $Ia\bar{3}d$ . Diffraction work at very low temperatures is needed to further address the symmetry relationships and the nature of hydrogen bonding in hydrogrossular. Low-temperature heat capacity measurements could also be useful in characterizing the nature of a possible phase transition.

It is clear from an analysis of the vibrational spectra that the

(O<sub>4</sub>H<sub>4</sub>) cluster is not a quasi-isolated structural unit similar, for example, to a SiO<sub>4</sub> tetrahedron in silicate garnet, but instead a topological construction following from the hydrogarnet structure. In terms of hydrogrossular's vibrational spectrum, it is the behavior of the individual OH groups and their interactions that strongly govern the lattice dynamic (i.e., thermodynamic) behavior of the O<sub>4</sub>H<sub>4</sub> groups. The line widths (FWHH) of the individual O-H stretching modes in the Raman spectra and the main IR OH envelope at 298 and 10 K are listed in Table 2. The modes are broad at room temperature and narrow considerably at low temperatures. O-H mode broadening with increasing temperature is interpreted to be a result of thermal anharmonicity and it is not related to some type of static structural disorder. The Raman modes, whose lines widths can be measured straightforwardly, are very narrow at low temperature and the FWHH of some of them may even be constrained by the spectral resolution of the spectrometer (i.e., 2 cm<sup>-1</sup> at 4 K). In the case of the IR spectra an exact determination of individual line widths is more difficult because of the strong overlap between O-H modes and the resulting uncertainty in the number of bands that are actually present. Nonetheless, we think that the FWHH's of most of the individual O-H bands lies between about 5 and 10 cm<sup>-1</sup>. Thus, they are broader than their Raman counterparts that have FWHH's between 2 and 5 cm<sup>-1</sup> at 10 K. At room temperature, however, the case is reversed and the  $F_{2g}$  Raman mode is broader (FWHH = 40 cm<sup>-1</sup>) than the single  $F_{1u}$  IR O-H band (FWHH = 33 cm<sup>-1</sup>). This behavior is unusual at first thought and needs explanation. First, it must be stated that a comparison of the line widths of  $F_{2g}$  Raman and  $F_{1u}$  IR O-H bands is valid, because both modes derive from the same  $B$ ,  $E(1)$ , and  $E(2)$  modes of a O<sub>4</sub>H<sub>4</sub> tetrahedron (Fig. 3). We can, thus, interpret the line width observations as follows: At 10 K all crystal modes (except zeroth-order vibrations) are nearly frozen and the motions of the hydrogen atoms are strongly damped, whereas at ambient temperature (e.g., 300 K) their thermal motions are considerably greater (see Lager et al. 2002). The time scales associated with IR and Raman spectroscopy are such that both give the natural line widths. The time scale related to IR absorbance lies between about 10<sup>-12</sup> and 10<sup>-14</sup> s and in the case of the excited vibrational state of an OH group (about 3650 cm<sup>-1</sup>) it should be closer to 10<sup>-14</sup> s. The time scale associated with Raman scattering, in comparison, is roughly 10<sup>-15</sup> s, which is less than the period of an O-H vibration. It follows that the  $F_{2g}$  Raman O-H stretching band should be broader than the  $F_{1u}$  IR band at room temperature, because the change in energy during scattering will be given by the "instantaneous" position of the H atom and the experimental FWHH reflects a "summation" of several very closely spaced scattering states of very slightly different energies. In comparison, the absorbance of an IR photon reflects more the time-averaged position of the H atom.

With regards to the broader issue of studying OH- and H<sub>2</sub>O in minerals, the results of this study have both technical and scientific implications. They show, as have other recent Raman and IR studies of H<sub>2</sub>O and its components in minerals (e.g., Kolesov and Geiger 2000, 2002), the need for making measurements at very low temperatures. This is necessary in some (many?) cases, because the light H atom can have large vibrational amplitudes at room temperature. Thus, some O-H modes are only observed at temperatures much below the temperature of liquid nitrogen (77

K). The low-temperature measurements give insightful information on the nature of hydrogen bonding, which can be stronger at lower temperature than at room temperature. In terms of the IR and Raman spectra of silicate garnets, and perhaps in other NAMS as well, a complete understanding of the nature of their OH<sup>-</sup> substitution mechanisms may, in some cases, require that their low temperature spectra be recorded and interpreted.

#### ACKNOWLEDGMENTS

We thank U. Cornelissen of the Institute of Inorganic Chemistry of Kiel University for making the IR measurements and L. Hallmann who undertook some of the synthesis experiments.

#### REFERENCES CITED

- Armbruster, T. and Lager, G.A. (1989) Oxygen disorder and the hydrogen position in garnet-hydrogarnet solid solution. *European Journal of Mineralogy*, 1, 363–369.
- Bell, D.R. and Rossman, G.R. (1992) Water in Earth's mantle: the role of nominally anhydrous minerals. *Science*, 255, 1391–1397.
- Cohen-Addad, C., Ducros, P., and Bertaut, E.F. (1967) Étude de la substitution du groupement SiO<sub>4</sub> par (OH)<sub>4</sub> dans les composés Al<sub>2</sub>Ca<sub>3</sub>(OH)<sub>12</sub> et Al<sub>2</sub>Ca<sub>3</sub>(SiO<sub>4</sub>)<sub>2.16</sub>(OH)<sub>3.36</sub> de type grenat. *Acta Crystallographica*, 23, 220–230.
- Flint, E.P., McMurdie, H.F., and Wells, L.S. (1941) Hydrothermal and X-ray studies of the garnet-hydrogarnet series and the relationship of the series to hydration products of portland cement. *Journal of Research of the National Bureau of Standards*, 27, 171–180.
- Foreman, D.W. Jr. (1968) Neutron and X-ray diffraction study of Ca<sub>3</sub>Al<sub>2</sub>(O<sub>4</sub>D<sub>4</sub>)<sub>3</sub>, a garnetoid. *Journal of Chemical Physics*, 48, 3037–3041.
- Geiger, C.A. and Armbruster, T. (1997) Mn<sub>3</sub>Al<sub>2</sub>Si<sub>3</sub>O<sub>12</sub> spessartine and Ca<sub>3</sub>Al<sub>2</sub>Si<sub>3</sub>O<sub>12</sub> grossular garnet: dynamical structural and thermodynamic properties. *American Mineralogist*, 82, 740–747.
- Geiger, C.A. and Kolesov, B.A. (2002) Microscopic-macroscopic relationships in silicates: Examples from IR and Raman spectroscopy and heat capacity measurements. In C.M. Gramaccioli, Ed., *Energy Modelling in Minerals*. *European Notes in Mineralogy*, 4, 347–387. 4<sup>th</sup> EMU School of Mineralogy, Budapest, Hungary.
- Geiger, C.A., Langer, K., Bell, D.R., Rossman, G.R., and Winkler, B. (1991) The hydroxide component in synthetic pyrope. *American Mineralogist*, 76, 49–59.
- Geiger, C.A., Stahl, A., and Rossman, G.R. (2000) Single-crystal IR- and UV/VIS-spectroscopic measurements on transition-metal-bearing pyrope: The incorporation of hydroxide in garnet. *European Journal of Mineralogy*, 12, 259–271.
- Harmon, K.M., Gabriele, J.M., and Nuttall, A.S. (1982) Hydrogen bonding. Part 14. Hydrogen bonding in the tetrahedral O<sub>4</sub>H<sub>4</sub><sup>+</sup> cluster in hydrogrossular. *Journal of Molecular Structure*, 82, 213–219.
- Hösch, A. and Langer, K. (1996) Single crystal MFTIR-spectra at various temperatures of synthetic end member garnets in the OH-valence vibrational region. *Physics and Chemistry of Minerals*, 23, 305–306.
- Kolesov, B.A. and Geiger, C.A. (1998) Raman spectra of silicate garnets. *Physics and Chemistry of Minerals*, 25, 142–151.
- — — (2000) A single-crystal Raman study of the orientation and vibrational states of molecular water in synthetic beryl. *Physics and Chemistry of Minerals*, 27, 557–564.
- — — (2002) Raman spectroscopic study of H<sub>2</sub>O in bikitaite: “One-dimensional” ice. *American Mineralogist*, 87, 1426–1431.
- Lager, G.A., Armbruster, T., and Faber, G. (1987) Neutron and X-ray diffraction study of hydrogarnet Ca<sub>3</sub>Al<sub>2</sub>(O<sub>4</sub>H<sub>4</sub>)<sub>3</sub>. *American Mineralogist*, 72, 756–765.
- Lager, G.A., Downs, R.T., Origlieri, M., and Garoutte, R. (2002) High-pressure single-crystal X-ray study of katoite hydrogarnet: Evidence for a phase transition from *Ia3d* → *I43d* symmetry at 5 GPa. *American Mineralogist*, 87, 642–647.
- Martin, R.F. and Donnay, G. (1972) Hydroxyl in the mantle. *American Mineralogist*, 57, 554–570.
- Matsyuk, S.S., Langer, K., and Hösch, A. (1998) Hydroxyl defects in garnets from mantle xenoliths in kimberlites of the Siberian platform. *Contributions to Mineralogy and Petrology*, 132, 163–179.
- Rossman, G.R. and Aines, R.D. (1991) The hydrous components in garnets: Grossular-hydrogrossular. *American Mineralogist*, 76, 1153–1164.
- Wilkins, R.W.T. and Sabine, W. (1973) Water content of some nominally anhydrous silicates. *American Mineralogist*, 58, 508–516.

MANUSCRIPT RECEIVED FEBRUARY 10, 2004

MANUSCRIPT ACCEPTED JANUARY 5, 2005

MANUSCRIPT HANDLED BY SIMON KOHN